The International Journal of Advanced Manufacturing Technology (2018) 97:2697–2702
https://doi.org/10.1007/s00170-018-2164-x

ORIGINAL ARTICLE

An investigation on surface functional parameters in ultrasonic-assisted grinding of soft steel

Haifeng Chen [1,2] · Jinyuan Tang [2] · Wen Shao [2] · Bo Zhao [3]

Received: 2 January 2018 / Accepted: 9 May 2018 / Published online: 19 May 2018

Abstract
In engineering applications, many surfaces are manufactured with some specific functional properties such as bearing, sealing, and lubricant retention capabilities. In order to figure out the characteristics of surfaces ground by ultrasonic-assisted grinding, surface bearing index S_{bi} and core fluid retention index S_{ci} were adopted in this study to investigate the effects of grinding velocity and ultrasonic vibration amplitude on the bearing and fluid retention properties of ground surfaces. Results indicated that the surface bearing index S_{bi} and core fluid retention index S_{ci} of ultrasonic-assisted grinding (UAG) were larger than those of common grinding (CG) under the same condition. The surface bearing index S_{bi} decreased with the increase of grinding velocity and increased with the increase of the ultrasonic vibration amplitude, while the core fluid retention index S_{ci} increased with both the grinding velocity and ultrasonic vibration amplitude. Ultrasonic-assisted grinding mechanisms were further explored to interpret these trends. The oscillation in the axial direction generates more overlaps, resulting in relatively flat-top surface. The oscillation in the radial direction generates more intermittent concave, thereby increasing the space for fluid.

Keywords Ultrasonic-assisted grinding · Surface bearing index · Core fluid retention index

1 Introduction

The ultrasonic-assisted grinding technique works by superimposing high frequency ($16-40$ kHz) and low amplitude ($2-30$ μm) vibration in the feed or cross-feed direction to the tool [1–3] or the workpiece [4–6]. It is applicable to both ductile and brittle materials. It was well documented that ultrasonic-assisted grinding could reduce thrust force and heat generation as well as improve surface quality under proper operating parameters compared with that of common grinding. Tawakoli and Azarhoushang [7] demonstrated that the thermal damage of the workpiece could be eliminated and the normal and tangential grinding forces reduced by 60–70 and 30–50%, respectively. Paknejad et al. [8] measured the temperature history and distribution of workpiece during ultrasonic-assisted dry creep feed up grinding and found out that the ultrasonic vibration resulted in a dramatic decrease in maximum temperature by 25.91% compared with common dry creep feed up grinding. Experimental results of Chen et al. [9, 10] on ultrasonic-assisted dry grinding of carbon steel showed a maximum reduction of 20% in surface roughness could be achieved compared with that of common dry grinding and had a better wear behavior by adopting Abbott curves. Wang et al. [11, 12] also reported that ultrasonic vibration frequency and amplitude had a significant influence on the material removal, grinding force, surface morphology, and roughness. It was found that higher amplitude and frequency tended to produce a better surface. The wear behavior of the diamond grinding wheel during the ultrasonic-assisted grinding was investigated by Wang et al. [13]. It was found that the cleavage fracture and macro-fracture of diamond grits resulted in higher active cutting edge density compared with that of common grinding, leading to a positive effect on the better grinding performance [14]. The grit protrusion height and the chip allowance space also increased by accelerating the removal rate of bond material with the aid of ultrasonic vibration [15].

✉ Jinyuan Tang
jytangcsu_312@163.com

[1] Hunan Province Key Laboratory of High Efficiency and Precision Machining of Difficult-to-Cut Materials, Hunan University of Science and Technology, Xiangtan 411201, Hunan, China

[2] State Key Laboratory of High Performance Complex Manufacturing, Central South University, Changsha 410083, Hunan, China

[3] School of Mechanical and Power Engineering, Henan Polytechnic University, Jiaozuo 454000, Henan, China

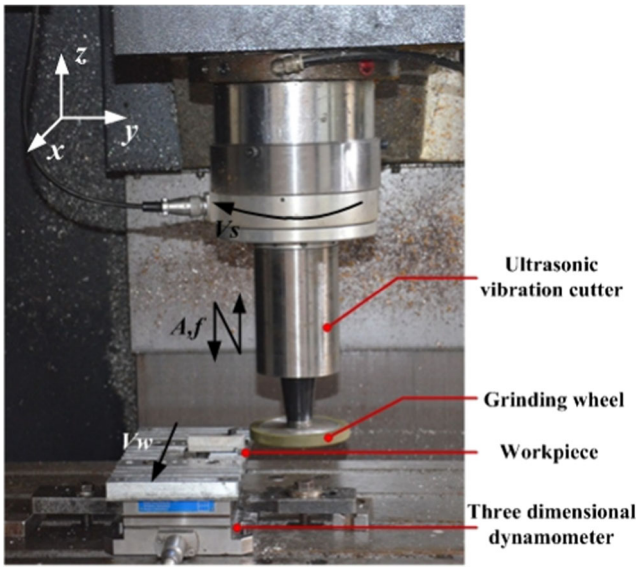

Fig. 1 Experimental set-up for ultrasonic-assisted dry grinding

As indicated by the literature review above, although the topography of the ground surfaces after UAG and CG have been extensively studied, most of the previous research have focused on surface roughness. Few studies have been conducted on the particular characteristics such as bearing, sealing, and lubricant retention capabilities of the ground surfaces especially in ultrasonic-assisted grinding, which are hard to be described through surface roughness. Functional analysis of surface with the surface bearing ratio was initiated by Abbott and Firestone. Later, the R_k parameter set, based on three-zone classification of the Abbott-Firestone curve, was formally standardized in DIN 4776. This parameter set is mainly used for characterizing surfaces with high stresses. These functional characterization methods are extensively used to classify different parts of the Abbott-Firestone curve into various functional zones. Dong et al. [16] defined surface bearing index S_{bi}, core fluid retention index S_{ci}, and valley fluid retention index S_{vi} to characterize different functional zones of surface topography. These parameters were widely used in automobile industry for characterizing cylinder surfaces. As revealed by Dong et al. [16], the larger S_{bi} indicated a good bearing property and the larger S_{ci} indicated a good fluid retention property. Therefore, functional parameters such as surface bearing index S_{bi} and core fluid retention index S_{ci} can be adopted as a novel approach to characterize the specific behaviors of the surfaces in ultrasonic-assisted grinding.

In this paper, an experimental platform was set up firstly for the ultrasonic-assisted grinding tests. Then, systematic experiments were conducted to investigate the influences of the vibration amplitude and the grinding velocity on the surface bearing index S_{bi} and core fluid retention index S_{ci}. Finally, the improvement mechanisms of the bearing and fluid retention property were further discussed from the view point of the effect of ultrasonic in different directions on the grain movement track.

Table 1 Mechanical properties of workpiece (12Cr2Ni4a)

Elastic modulus (GPa)	Density (kg/m^3)	Poisson's ratio	HV
207	7.84×10^3	0.298	210

Table 2 Experimental conditions

Conditions	Feature
Ultrasonic vibration	Frequency: $f = 25$ kHz
	Amplitude: 4, 7, and 10 μm
Grinding wheel	CBN: 120 M
	Concentration: 100%
	Diameter: $d_s = 100$ mm
	Width: 10 mm
Grinding parameters	Feed speed: $V_w = 300$ mm/min
	Spindle speed: $v_s = 400$, 800, 1200, 1600, 2000, 2400 r/min
	Grinding depth: $a_p = 10$ μm
Coolant	Dry grinding
Workpiece	12Cr2Ni4A(L16×W9×T9 mm)

2 Experimental details

The grinding tests of this research were performed on a three-axis NC milling machine with the conventional main spindle replaced with an ultrasonic unit. The processing principle of UAG is schematically illustrated in Fig. 1. During the grinding process, besides the rotational movement from the spindle, vertical ultrasonic vibration with frequency f of 25 kHz and amplitudes A around 4, 7, and 10 μm is transmitted to the grinding wheel from the ultrasonic vibration source. At the lower end of the spindle, a resin-bonded 120# CBN grinding wheel with a

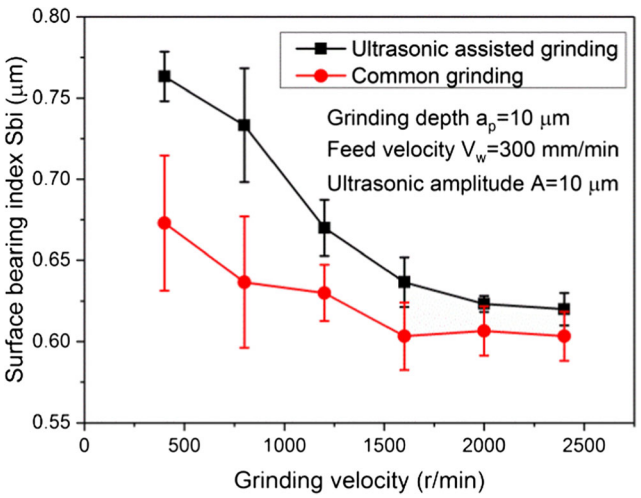

Fig. 2 Effect of grinding velocity on S_{bi}

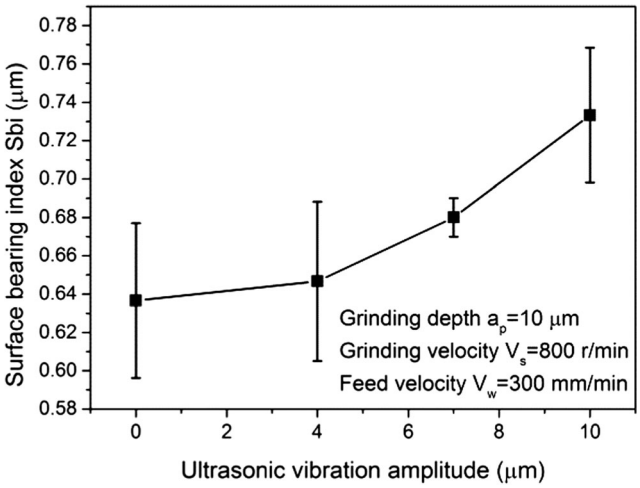

Fig. 3 Effect of ultrasonic amplitude on S_{bi}

diameter of 100 mm was fixed, which was manufactured by Zhengzhou Research Institute for Abrasives & Grinding Co. Ltd. A plate-shaped specimen of 12Cr2Ni4A steel (tempering at 140 °C) with dimensions of L16×W9×T9 mm was used as the workpiece. The main mechanical properties of the workpiece are listed in Table 1. The experimental conditions are listed in Table 2.

Wheel dressing was carried out prior to each group using a silicon carbide roller (GC120H7V) with feed rate, spindle speed, and dressing depth of 100 mm/min, 2000 rpm, and 30 μm respectively. Common grinding tests were performed by switching off the ultrasonic generator.

After the grinding tests, the sample was ultrasonically cleaned for 15 min in anhydrous alcohol. A white-light interferometer (NT9100 by Wyko, Co., Ltd) was employed to measure the three-dimensional surface roughness parameters. To ensure the reliability of the test data, three tests were carried out where each set of the process parameters was used to get the average values.

3 Results and discussions

Figure 2 shows the influences of grinding velocity and ultrasonic vibration on surface bearing index S_{bi}. The grinding depth, feed velocity, and ultrasonic vibration amplitude were set as 10 μm, 300 mm/min, and 10 μmrespectively. It can be seen from Fig. 2 that the surface bearing index S_{bi} for UAG and CG decreases with the increase of the grinding velocity. This is probably due to the surface bearing index S_{bi} that is proportional to the surface roughness S_q and inversely proportional to the surface heights at 5% bearing area $\eta_{0.05}$ as defined in the Appendix. The increase of grinding speed generally improves the surface quality. Thus, the surface roughness S_q decreases with the increase of grinding velocity. And $\eta_{0.05}$ is correlative to the height distribution and topographic feature. Typically, the changes of height distribution and topographic feature are small for the same processing technology. Therefore, the surface bearing index S_{bi} decreases with the increase of the grinding velocity. The results also show that UAG exerts certain effect in increasing the surface bearing index S_{bi} at the low grinding velocity, which indicates the surface produced by UAG has a better bearing property. As shown in Fig. 3, under the same grinding velocity, S_{bi} increases with the increase of ultrasonic vibration amplitude. The main reason for the abovementioned results is that the ultrasonic vibration changes the individual grain traces. The grinding trace of UAG is a three-dimensional curved line that looks like a spatial sinusoidal curve. Its length would be longer than that of CG, indicating that the grits of UAG would

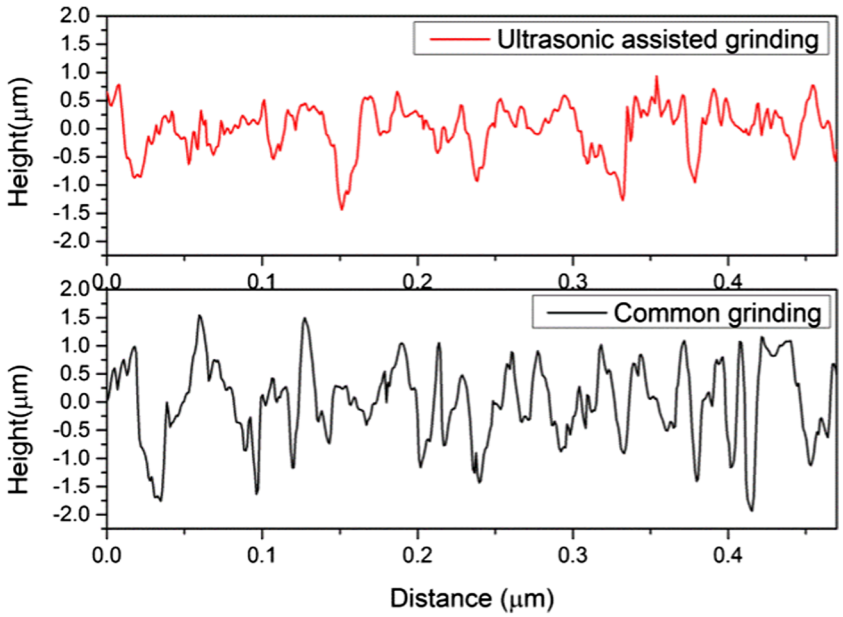

Fig. 4 Surface profiles of the ground workpiece in CG and UAG (grinding velocity = 800 rpm, grinding depth = 10 um, feed = 300 mm/min, and ultrasonic amplitude A = 10 um)

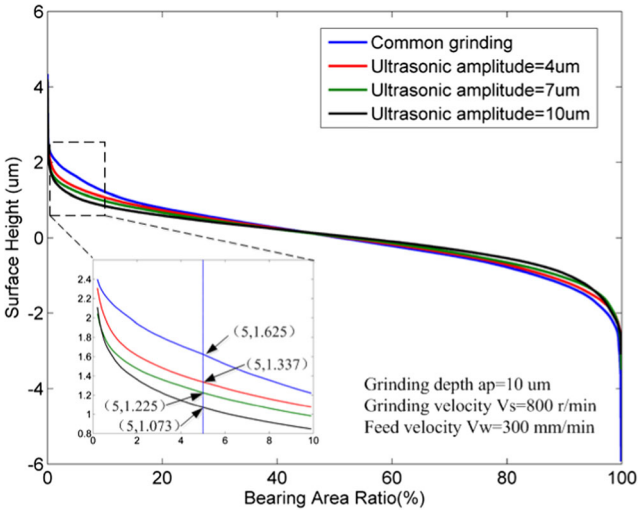

Fig. 5 Surface height of the ground workpiece in CG and UAG with various amplitudes

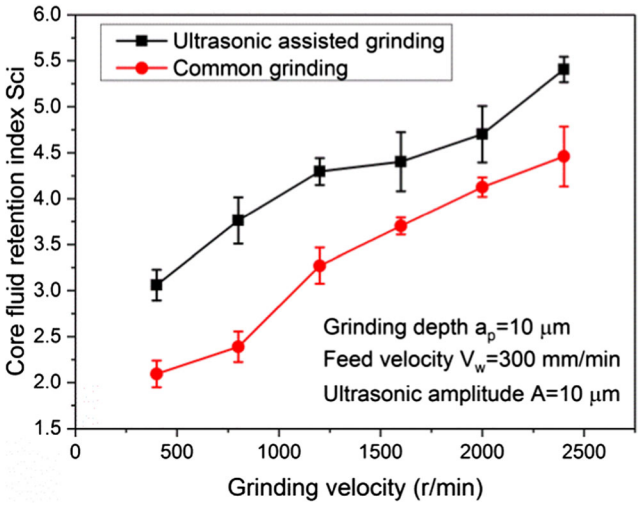

Fig. 7 Effect of grinding velocity on S_{ci}

interact with each other and generate more overlaps of the material removal than that of CG. Thus, less grinding marks and better workpiece surface quality would be achieved. Figure 4 presents the two-dimensional profiles of the ground surface perpendicular to the grinding direction in CG and UAG with grinding depth, wheel speed, and feed velocity of 10 μm, 800 r/min, and 300 mm/min. It can be found that the profile produced by CG has spiky ridges while the profile produced by UAG has a relatively flat top. In order to further understand the impact of the topographic feature on $\eta_{0.05}$, the surface height at the 5% bearing area in CG and UAG with different ultrasonic amplitude is shown in Fig. 5. As shown in Fig. 5, the surface height at the 5% bearing area for CG is 1.625 μm, which is much higher than that of UAG. It may due to the relatively flat-top surface has a fast increase rate of the bearing area ratio from 0 bearing to 5%. This leads to a lower surface bearing index of CG. Moreover, the topographic feature is related to the effect of overlapping caused by the ultrasonic vibration, that is, greater ultrasonic amplitude can cause more obvious overlapping. This might be the reason why $\eta_{0.05}$ decreases with the increase of the ultrasonic amplitude under the same conditions, resulting in an increase of surface bearing index S_{bi}. However, with the increase of the grinding velocity, the length of UAG and CG for a single grain tends to equalize, as shown in Fig. 6. Then, the chance of the overlapping of the trajectories would reduce. Therefore, the improving effect of the ultrasonic vibration on the surface bearing index S_{bi} gradually weakens with the increase of the grinding velocity.

The influences of the grinding velocity and ultrasonic vibration on core fluid retention index S_{ci} were also investigated and shown in Figs. 7 and 8. As can be seen from Fig. 7, a similar trend is observed for the core fluid retention index S_{ci} of UAG and CG. It is found that the value of S_{ci} rises against

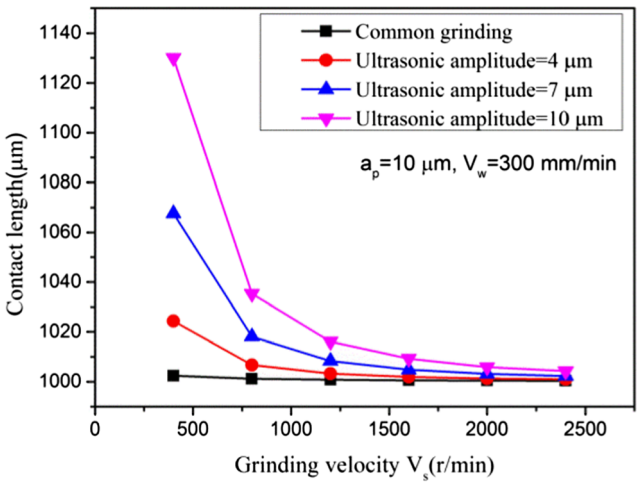

Fig. 6 Contact length versus grinding velocity for different ultrasonic amplitudes

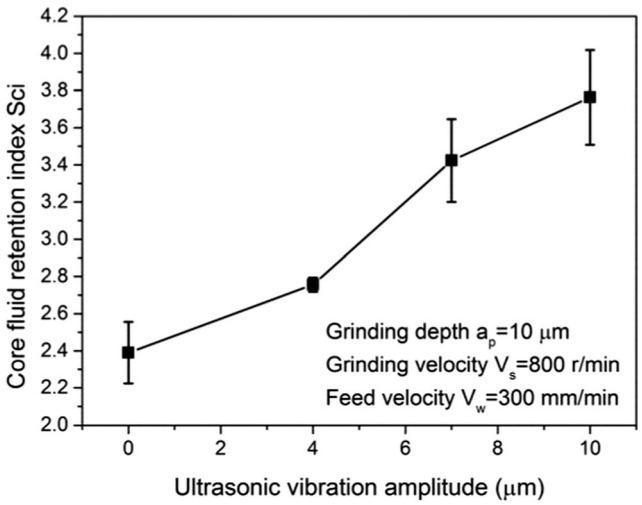

Fig. 8 Effect of ultrasonic amplitude on S_{ci}

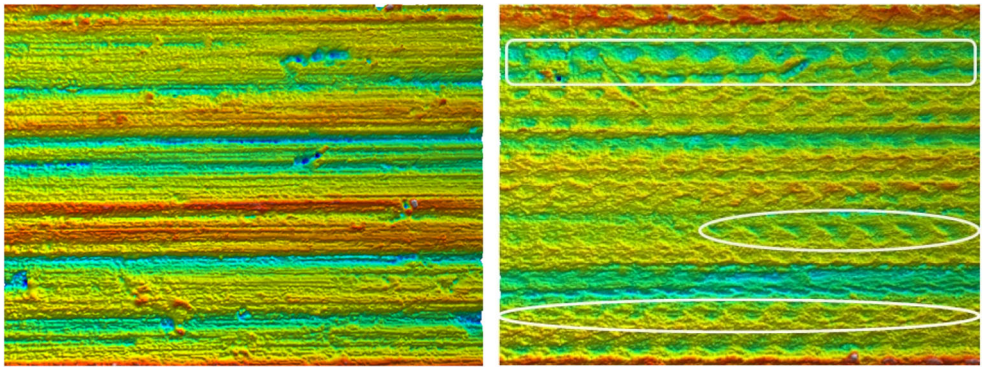

Fig. 9 Surface topography of the ground workpiece in CG and UAG

the grinding velocity. It may be due to the S_{ci} is inversely proportional to the S_q. As mentioned before, the S_q decreases with the increase of grinding velocity. Then, the value of S_{ci} rises against the grinding velocity. By comparison, it is found that the S_{ci} in UAG is larger than that in CG. Besides, as shown in Fig. 8, under the same grinding velocity, S_{ci} increases with the increase of ultrasonic vibration amplitude. As revealed by Dong et al. [16], the larger S_{ci} indicated a good fluid retention property in the core zone. This indicates that the surface produced by UAG is more beneficial for the lubricating oil stored in the concave grove to lubricate the friction pairs. The main reason for the abovementioned results is that pure longitudinal waves can only exist in solids where the dimensions are very large compared with the longitudinal wavelength. If not, due to the Poisson effect, another ultrasonic vibration is simultaneously generated in the radial direction at the same frequency but with a much smaller amplitude [17, 18]. And the amplitude in the radial direction is proportional to the diameter of the grinding wheel [19]. In the current work, to verify this statement, the vibration amplitude of the grinding wheel in the radial and axial direction was measured using a laser displacement sensor (LK-G10 by KEYENCE). The test results confirmed that the ultrasonic amplitude was about 3 μm in the radial direction and about 10 μm in the axial direction. Therefore, the ultrasonic-assisted grinding using a large diameter grinding wheel is just the combination of axial ultrasonic-assisted grinding and radial ultrasonic-assisted grinding. Due to the oscillation in the radial direction, the tool moves leftward and rightward alternatively in the cutting process, which leads the depth of grinding in UAG to vary periodically, resulting in a relative greater maximum depth compared with that of CG. It can be observed from the ground surfaces shown in Fig. 9 that the ground surface after CG consists of numerous small and straight grinding grooves while the grinding grooves in UAG are in a sinusoidal shape and feature intermittent concaves owing to the ultrasonic vibration in the radial direction (the area outlined in white). These intermittent concaves increase the space for fluid, which indicates that surfaces of this kind have a good fluid retention property. Besides, the depth of intermittent concave is related to the ultrasonic vibration amplitude so that greater ultrasonic action can cause deeper concaves, leading to an increase of the core fluid retention index S_{bi}.

4 Conclusions

In this study, surface bearing index S_{bi} and core fluid retention index S_{ci} were employed to investigate the effects of grinding velocity and vibration amplitudes on the bearing and fluid retention properties of ground surfaces of CG and UAG. The main findings can be summarized as follows:

(1) The surface bearing index S_{bi} value in UAG is larger than that in CG. It decreases with the increase of the grinding velocity and increases with the increase of the ultrasonic vibration amplitude, which indicates that the ground surface generated by UAG has a better bearing property.
(2) The core fluid retention index S_{ci} value in UAG is also larger than that in CG. It increases with the increase of the grinding velocity and increases with the increase of the ultrasonic vibration amplitude, which indicates that the ground surface generated by UAG also has a better fluid retention property.

Funding information The authors gratefully thank the support of the National Natural Science Foundation of China (NSFC) through Grant Nos. 51535012, 51605160, and U1604255, the support of the Key research and development project of Hunan province through Grant No. 2016JC2001, and the open Research Fund of Key Laboratory of High Performance Complex Manufacturing, Central South University (No. Kfkt2016-8).

Appendix

The surface bearing index S_{bi} is a parameter used to indicate the bearing property of a surface. It is defined as the ratio of the RMS deviation over the surface height at 5% bearing area, as

$$S_{bi} = \frac{S_q}{\eta_{0.05}} \tag{1}$$

where S_q is the root-mean-square deviation of surface topography and $\eta_{0.05}$ is the surface heights at 5% bearing area. A larger surface bearing index indicates a good bearing property.

The core fluid retention index S_{ci} is a parameter used to indicate the fluid retention property in the core zone. It is defined as the ratio of the void volume per unit sampling area at the core zone over the RMS deviation, i.e.,

$$S_{ci} = \frac{1}{S_q} \frac{V_v(h_{0.05}) - V_v(h_{0.08})}{(M-1)(N-1)\Delta x \Delta y} \quad (2)$$

where $V_v(h_{0.05})$ is the void volume of the surface heights, $h_{0.05}$, M, and N represent the number of sampling points in the x and y directions, and Δx and Δy are the sampling intervals.

References

1. Li C, Zhang F, Meng B, Liu L, Rao X (2016) Material removal mechanism and grinding force modelling of ultrasonic vibration assisted grinding for SiC ceramics. Ceram Int 43(3)
2. Gong H, Fang FZ, Hu XT (2010) Kinematic view of tool life in rotary ultrasonic side milling of hard and brittle materials. Int J Mach Tools Manuf 50(3):303–307. https://doi.org/10.1016/j.ijmachtools.2009.12.006
3. Qi H, Wen D, Lu C, Li G (2016) Numerical and experimental study on ultrasonic vibration-assisted micro-channelling of glasses using an abrasive slurry jet. Int J Mech Sci 110:94–107
4. Abdullah A, Sotoodezadeh M, Abedini R, Fartashvand V (2013) Experimental study on ultrasonic use in dry creep-feed up-grinding of aluminum 7075 and steel X210Cr12. Int J Precis Eng Manuf 14(2):191–198. https://doi.org/10.1007/s12541-013-0027-9
5. Molaie MM, Akbari J, Movahhedy MR (2016) Ultrasonic assisted grinding process with minimum quantity lubrication using oil-based nanofluids. J Clean Prod 129:212–222
6. Chen H, Tang J, Zhou W (2013) An experimental study of the effects of ultrasonic vibration on grinding surface roughness of C45 carbon steel. Int J Adv Manuf Technol 68(9–12):2095–2098. https://doi.org/10.1007/s00170-013-4824-1
7. Tawakoli T, Azarhoushang B (2008) Influence of ultrasonic vibrations on dry grinding of soft steel. Int J Mach Tools Manuf 48(14):1585–1591. https://doi.org/10.1016/j.ijmachtools.2008.05.010
8. Paknejad M, Abdullah A, Azarhoushang B (2017) Effects of high power ultrasonic vibration on temperature distribution of workpiece in dry creep feed up grinding. Ultrason Sonochem 39:392–402. https://doi.org/10.1016/j.ultsonch.2017.04.029
9. Chen H, Tang J, Lang X, Huang Y, He Y (2014) Influences of dressing lead on surface roughness of ultrasonic-assisted grinding. Int J Adv Manuf Technol 71(9–12):2011–2015. https://doi.org/10.1007/s00170-014-5636-7
10. Chen H, Tang J (2016) Influence of ultrasonic assisted grinding on Abbott-Firestone curve. Int J Adv Manuf Technol 86(9–12):2753–2757. https://doi.org/10.1007/s00170-016-8370-5
11. Wang Y, Lin B, Wang S, Cao X (2014) Study on the system matching of ultrasonic vibration assisted grinding for hard and brittle materials processing. Int J Mach Tools Manuf 77:66–73. https://doi.org/10.1016/j.ijmachtools.2013.11.003
12. Wang Y, Lin B, Cao X, Wang S (2014) An experimental investigation of system matching in ultrasonic vibration assisted grinding for titanium. J Mater Process Technol 214(9):1871–1878
13. Wang Q, Zhao W, Liang Z, Wang X, Zhou T, Wu Y, Jiao L (2017) Investigation of diamond wheel topography in elliptical ultrasonic assisted grinding (EUAG) of monocrystal sapphire using fractal analysis method. Ultrasonics 84:87–95. https://doi.org/10.1016/j.ultras.2017.10.012
14. Liang Z, Wang X, Wu Y, Xie L, Liu Z, Zhao W (2012) An investigation on wear mechanism of resin-bonded diamond wheel in elliptical ultrasonic assisted grinding (EUAG) of monocrystal sapphire. J Mater Process Technol 212(4):868–876. https://doi.org/10.1016/j.jmatprotec.2011.11.009
15. Shen JY, Wang JQ, Jiang B, Xu XP (2015) Study on wear of diamond wheel in ultrasonic vibration-assisted grinding ceramic. Wear 332-333:788–793. https://doi.org/10.1016/j.wear.2015.02.047
16. Dong WP, Sullivan PJ, Stout KJ (1994) Comprehensive study of parameters for characterising three-dimensional surface topography III: parameters for characterising amplitude and some functional properties. Wear 178:29–43
17. Cao J, Wu Y, Lu D, Fujimoto M, Nomura M (2014) Material removal behavior in ultrasonic-assisted scratching of SiC ceramics with a single diamond tool. Int J Mach Tool Manu 79(4):49–61
18. Li S, Wu Y, Nomura M (2016) Effect of grinding wheel ultrasonic vibration on chip formation in surface grinding of Inconel 718. Int J Adv Manuf Technol 86(1):1113–1125
19. Cang-Leh C (1994) Wave effects of ultrasonic vibration on machining. The Pennsylvania State University, State College